Available online at www.sciencedirect.com
ScienceDirect
Journal of Molecular Catalysis A: Chemical 274 (2007) 42–49
JOURNAL OF MOLECULAR CATALYSIS A: CHEMICAL
www.elsevier.com/locate/molcata

Dehydrogenation of hydroxymatairesinol to oxomatairesinol over carbon nanofibre-supported palladium catalysts

Heidi Markus [a], Arie J. Plomp [b], Thomas Sandberg [c], Ville Nieminen [a], Johannes H. Bitter [b], Dmitry Yu. Murzin [a,*]

[a] *Laboratory of Industrial Chemistry, Process Chemistry Centre, Åbo Akademi University, Biskopsgatan 8, FI-20500 Turku, Finland*
[b] *Department of Inorganic Chemistry and Catalysis, Utrecht University, P.O. Box 80083, Utrecht 3508 TB, The Netherlands*
[c] *Department of Physical Chemistry, Åbo Akademi University, Porthansgatan 3-5, FI-20500 Turku, Finland*

Received 5 March 2007; accepted 17 April 2007
Available online 22 April 2007

Abstract

Dehydrogenation of the naturally occurring lignan hydroxymatairesinol to oxomatairesinol was performed over carbon nanofibre supported palladium catalysts (Pd/CNF) under nitrogen flow at 70 °C. To study the influence of support acidity on the catalyst performance, the amount of acid sites on the catalysts surface was varied by heat-treatment in nitrogen flow. It was concluded that both activity and selectivity to oxomatairesinol increased when the concentration of acid sites increased. The selectivity to oxomatairesinol was over 70% (at 4 h with 50% yield) when 2-propanol was used as solvent and the major by-product was 7-iso-propoxymatairesinol resulting from interactions with the solvent. In 2-pentanol, the selectivity increased to 90% (at 4 h with 50% yield). It was demonstrated that only one of the two diastereomers of hydroxymatairesinol preferentially yields oxomatairesinol. Quantum chemical calculations were performed as an attempt to explain this behaviour and to understand the role of acid sites.

Keywords: Dehydrogenation; Acidity; Palladium; Carbon nanofibres; Quantum chemical calculations

1. Introduction

Lignans, a group of plant phenols consisting of two β–β-linked cinnamic acid residues, can be found in many different plant parts [1]. Large amounts of the lignan hydroxymatairesinol (HMR) can be extracted from Norway spruce (*Picea abies*) knots, i.e. the part of the branch that is embedded in the stem [2]. There are two diastereomers of hydroxymatairesinol, (7*R*,8*R*,8′*R*)-(−)-7-allo-hydroxymatairesinol (HMR 1) and (7*S*,8*R*,8′*R*)-(−)-7-hydroxymatairesinol (HMR 2), and the ratio between the isomers can vary. Other lignans can be synthesized using HMR as starting material [3–8]. Recent studies have shown that several lignans have anticarcinogenic [9] and antioxidative [10–12] effects.

The lignan 7-oxomatairesinol (oxoMAT) could be an interesting alternative for pharmaceutical or technical purposes. Kawamura et al. [13] reported the formation of oxoMAT from HMR by light-irradiation, while Eklund and Sjöholm [4] used the oxidising agent 2,3-dichloro-5,6-dicyano-1,4-benzoquinone (DDQ) to obtain oxoMAT from HMR. We have earlier reported the possibility to obtain oxoMAT through dehydrogenation of HMR at anaerobic conditions using palladium supported by a beta-zeolite [7]. In this work, we have studied the dehydrogenation of HMR to oxoMAT using carbon nanofibre supported palladium catalysts. Carbon nanofibres (CNF) are synthetic carbon materials grown by decomposition of carbon-containing gases on small metal particles. Reviews concerning CNF [14,15] describe the synthesis and properties of these materials in detail. The CNF are pure (after the growth catalyst has been removed), mechanically strong [16] and of mesoporous nature, which makes them suitable support materials in liquid-phase reactions [17]. Activated carbons

* Corresponding author. Tel.: +358 2 215 4985; fax: +358 2 215 4479.
E-mail address: dmurzin@abo.fi (D.Yu. Murzin).

1381-1169/$ – see front matter © 2007 Elsevier B.V. All rights reserved.
doi:10.1016/j.molcata.2007.04.025

are frequently used as catalyst support materials in liquid-phase reactions. As the properties of activated carbons can be difficult to control resulting in poor reproducibility and the microporous nature causes diffusion problems, CNF could replace the use of activated carbons in fine chemical production.

In dehydrogenation reactions, several methods can be utilized to remove the hydrogen. One of the most common methods is to use oxygen, called oxidative dehydrogenation [18,19]. Hydrogen acceptors such as styrene [20,21], cyclohexene, vinyl acetate, methyl acrylate, 1-hexene, cyclopentene and methyl vinyl ketone [21] have also been applied in dehydrogenation reactions. Zaccheria et al. [20] reported that in absence of hydrogen acceptor, equilibrium between dehydrogenation and hydrogenation was reached in the anaerobic oxidation of secondary alcohols over Cu/Al_2O_3, but it was also mentioned that venting the reactor at regular times made it possible for the reaction to go to completion [20].

In this work, the influence of support acidity on the activity and the selectivity to oxoMAT was studied. The palladium was deposited on herringbone CNF, which were oxidised in concentrated nitric acid. The catalyst was then subjected to heat-treatment to vary the amount of acid sites. The reaction was carried out under nitrogen flow to remove the hydrogen formed in the reaction. The overall process safety increases when nitrogen is used instead of oxygen. Many hydrogen acceptors or the products formed when hydrogen acceptors are used can have a negative impact on the environment. In the production of anticarcinogenic and antioxidative foods or pharmaceuticals, extra additives are unwanted and green solvents should be used.

2. Experimental

2.1. Synthesis of carbon nanofibre supported palladium catalysts

The synthesis of the Pd/CNF catalyst is described in detail in Ref. [22]. The preparation of the Ni/SiO_2 growth catalyst and the synthesis of the carbon nanofibres (CNF) are described in Ref. [23]. The deposition of palladium on CNF was performed via an ion adsorption method according to Ref. [24]. The Pd/CNF catalyst was reduced in hydrogen flow (96 mL/min) and nitrogen flow (480 mL/min) at 250 °C (ramp 5 °C/min) and 1.33 bar for 2 h. The catalyst was sieved (25–90 μm) and stored in static air for further use. The Pd/CNF obtained will be indicated as Pd/CNF-ox in the following text.

To vary the amount of acid sites on the support material, some of the acidic groups on the Pd/CNF-ox catalyst were removed by heat-treatment in nitrogen flow at 300 °C, 400 °C or 500 °C for 2 h (ramp 5 °C/min). The resulting products will be indicated as Pd/CNF-300, Pd/CNF-400 or Pd/CNF-500. The concentration of acid sites decreased in the order Pd/CNF-ox > Pd/CNF-300 > Pd/CNF-400 > Pd/CNF-500. The characterization of the Pd/CNF catalysts is described in Ref. [22].

2.2. Dehydrogenation of hydroxymatairesinol

Hydroxymatairesinol was isolated from Norway spruce knots as described in Ref. [6]: the knots were ground and extracted in acetone–water mixture. The extract was concentrated in a rotary evaporator and then purified by flash chromatography.

Experiments were performed under atmospheric pressure in a 200 mL glass reactor equipped with a heating jacket, a re-flux condenser, oil lock, pitched-blade turbine, and stirring baffles. The catalyst was pre-activated *in situ* by hydrogen (AGA, 99.999%) flow (100 mL/min) at 100 °C in 1 h (including heating time), after which the reactor was cooled down to the reaction temperature 70 °C under nitrogen (AGA, 99.999%) flow (100 mL/min). The reactant solution, consisting of hydroxymatairesinol dissolved in 100 mL 2-propanol (J.T. Baker, 99.5%) or 2-pentanol (Fluka, >98.0%), was deoxygenated by nitrogen flow (100 mL/min) for 10 min in a glass tube. After pouring the reactant solution into the reactor, the stirring was started at reaction time set to zero and the first sample was withdrawn (nitrogen flow 100 mL/min).

Samples were taken at different time intervals and analysed by a gas chromatograph (GC) as described in Ref. [7]. The samples were silylated prior to analysis using *N*,*O*-bis(trimethylsilyl)trifluoro-acetamide (BSTFA, 98%, Fluka), trimethylchlorosilane (TMCS, 98%, Acros Organics), and pyridine (99.0%, J.T. Baker).

2.3. Computational methods

In order to evaluate whether the different behaviour in the reaction of HMR 1 and HMR 2 is due to the intrinsic differences of the two molecules, charges, bond orders and protonation energies were evaluated computationally. The conformations of HMR 1 and HMR 2 were taken from the work of Taskinen et al. [25]. Mulliken and Löwdin charges, electrostatic potential fit (ESP) and bond orders were calculated with the GAMESS software [26] by using Hartree-Fock (HF) theory [27] with the basis set 6-31G* [28–30].

As the protonation [6] and deprotonation can be crucial for the reactions, protonated and deprotonated (abstraction of proton from the hydroxyl group) HMR 1 and HMR 2 were studied in detail. The protonated structures were optimized using the TURBOMOLE program package version 5.8 [31–33] and density functional theory (DFT) with the BP86 exchange-correlation functional [34,35] in combination with the multipole accelerated resolution of identity (MARI-*J*) approximation [36–38] and the triple zeta valence plus polarization TZVP basis set [39].

The most stable protonated, deprotonated and neutral structures were optimized with the B3LYP hybrid exchange-correlation functional [34,40,41] with the TZVP basis set. Vibrational analysis was carried out for the B3LYP/TZVP optimized structures in order to prove that all optimized structures are real minima on the potential energy surface and to obtain the thermodynamic contributions. Frequencies were scaled with a factor of 0.9614 [42] when calculating the thermodynamic contributions at 25 °C. When the stabilities at the B3LYP/TZVP

level are compared in the text below, we are always referring to the Gibbs' free energies (ΔG, 25 °C).

3. Results and discussion

3.1. Catalyst activity and selectivity

The reaction scheme is illustrated in Fig. 1. The desired product was oxomatairesinol (oxoMAT) formed through dehydrogenation of hydroxymatairesinol (HMR). Side reactions were hydrogenolysis of HMR to matairesinol (MAT) and etherification of HMR to 7-iso-propoxymatairesinol (7-i-propoxyMAT, two isomers). 7-i-propoxyMAT was formed through interactions with the solvent 2-propanol.

In Fig. 2a the yield of oxoMAT versus time for Pd/CNF with varied amount of acid sites is presented. The catalyst with largest amount of acid sites (Pd/CNF-ox) gave the highest yield of oxoMAT and the yield decreased when the acidity of the support material decreased. This implies that acidic groups assist removal of hydrogen from HMR. Such behaviour can be attributed either to intrinsic features of acidic support or by alteration of metal function due to the modified environment. The interaction between CNF and metal can be considered as rather weak and consequently we focus on the direct influence of acid sites on the dehydrogenation reaction.

The selectivity to oxoMAT decreased when the amount of acid sites decreased as illustrated by Fig. 2b, where the selectivity is given as a function of conversion of HMR. The selectivity decreased with conversion, which is not typical for conventional parallel reactions. There are several possible explanations for this. The conversion is calculated using the change in total HMR concentration, but the two isomers react differently and also isomerization between the isomers can take place, which could change the product distribution during the reaction. Moreover, the dehydrogenation and hydrogenolysis [6,7,22] require both metal and acid sites, while etherification can take place on acid sites only and therefore a change in the number of metal sites due to deactivation would affect the product distribution.

The HMR 2-to-HMR 1 ratio was 2 in the beginning of the experiments and remained constant during the reaction when catalysts Pd/CNF-400 and Pd/CNF-500 were used (Fig. 2c). For the catalysts having the largest amounts of acid sites, Pd/CNF-ox and Pd/CNF-300, the ratio decreased with conversion.

Fig. 3a shows the conversion after 4 h of reaction versus concentration of acid sites for the four Pd/CNF catalysts (the detailed information about the measuring of acid sites is found in Ref. [22]). It is clear that the activity increased when the acidity increased. Fig. 3b shows the yield of oxoMAT and by-products after 4 h of reaction versus concentration of acid sites. The yield of MAT decreased when the concentration of acid sites decreased. Since the dehydrogenation of HMR to oxoMAT gives hydrogen, which can be used in the hydrogenolysis of HMR to MAT, it is logical that when the amount of oxoMAT is smaller also formation of MAT is less pronounced. The yield of the two 7-i-propoxyMAT isomers was highest for the two catalysts having the lowest concentration of acid sites. The isomers are here called propoxyMAT 1 and propoxyMAT 2, based on their elution order on the GC, as no further study was made to determine their stereochemistry. 7-i-propoxyMAT was formed easily using CNF without metal. It is conventionally assumed, that reaction rate in etherification reactions is proportional to the concentration of acid sites. For instance, Parra et al. [43] studied the activity of several styrene-divinylbenzene ion-exchange resin catalysts in the etherification of isobutylene with methanol and concluded that catalysts with higher acidic capacity were more active in the etherification reaction. Somewhat surprisingly the yield of 7-i-propoxyMAT decreased with the acidity of the Pd/CNF catalysts. However, it is difficult to determine the

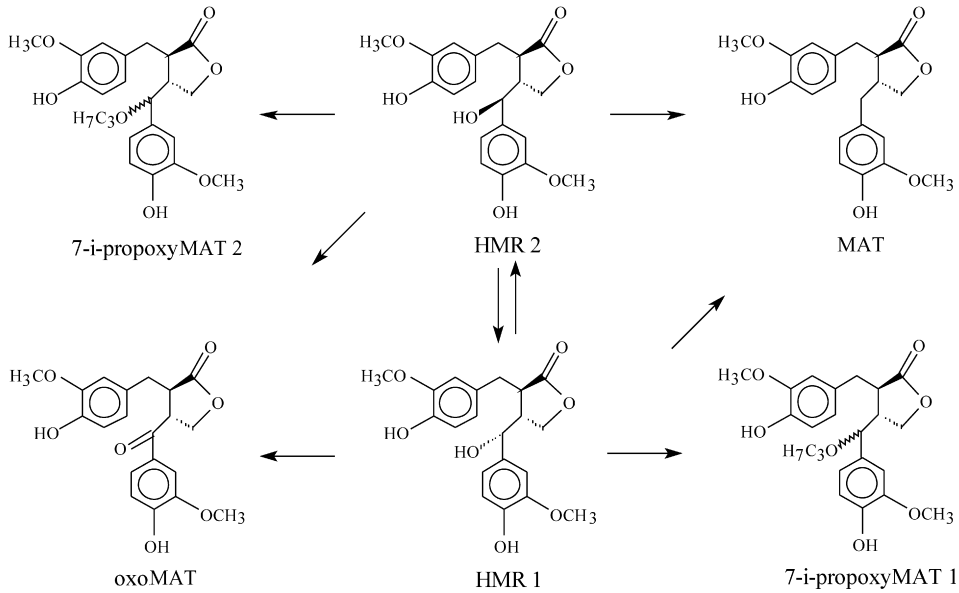

Fig. 1. Dehydrogenation of 7-hydroxymatairesinol (HMR) to 7-oxomatairesinol (oxoMAT), hydrogenolysis of HMR to matairesinol (MAT), and etherification of HMR to 7-iso-propoxymatairesinol (7-i-propoxyMAT).

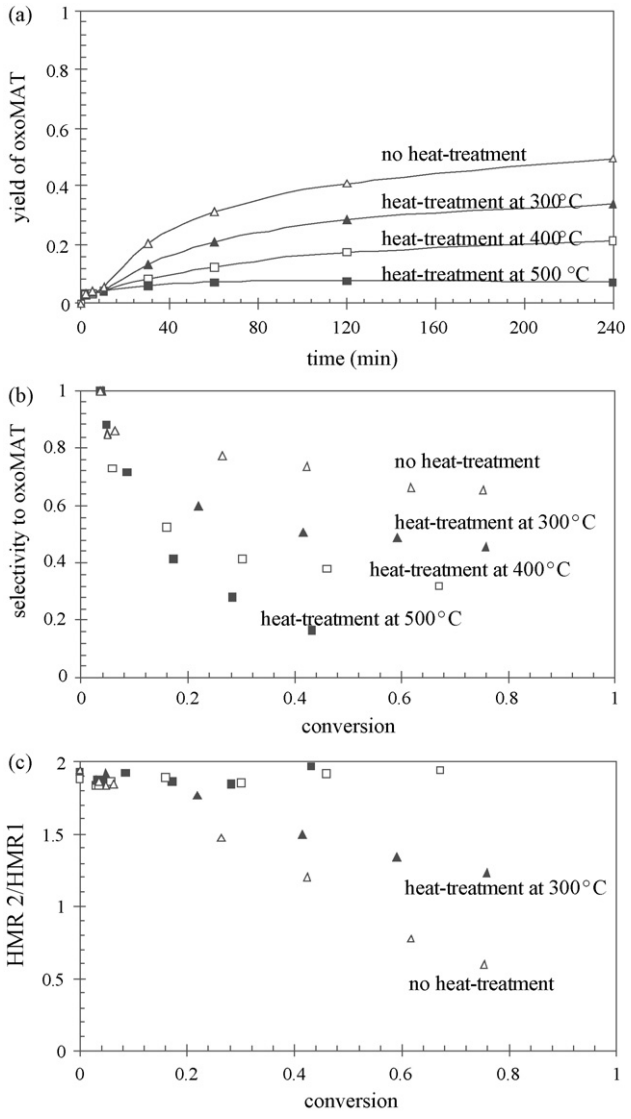

Fig. 2. Dehydrogenation of HMR to oxoMAT over CNF supported palladium catalysts: (△) no heat-treatment (Pd/CNF-ox), (▲) treatment in nitrogen-flow at 300 °C (Pd/CNF-300), (□) treatment in nitrogen-flow at 400 °C (Pd/CNF-400), and (■) treatment in nitrogen-flow at 500 °C (Pd/CNF-500). (a) Yield oxoMAT vs. time, (b) selectivity to oxoMAT vs. conversion, and (c) HMR 2-to-HMR 1 ratio vs. conversion. Conditions: 500 mg 0.99% Pd/CNF catalyst, 0.27 mmol HMR, 100 mL 2-propanol, 70 °C, 100 mL/min N_2-flow (atmospheric pressure), the HMR 2/HMR 1 initial ratio was 2.

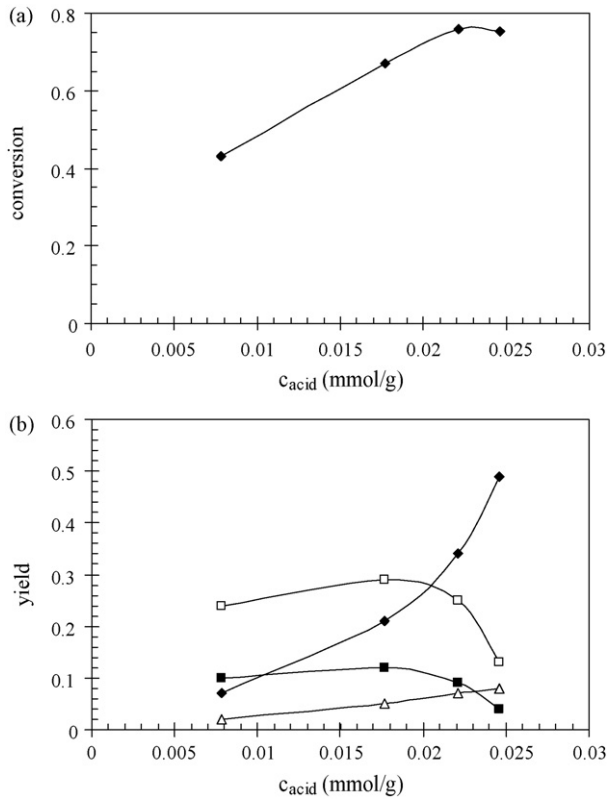

Fig. 3. Dehydrogenation of HMR to oxoMAT: (a) conversion in 4 h vs. concentration of acid sites on Pd/CNF catalyst and (b) yield in 4 h vs. concentration of acid sites. (♦) 7-Oxomatairesinol, (□) 7-iso-propoxymatairesinol 1, (■) 7-iso-propoxymatairesinol 2 and (△) matairesinol. Conditions are the same as in Fig. 2.

relationship between etherification reaction rate and concentration of acid sites, since the main reaction, dehydrogenation of HMR, depends strongly on the acid site concentration.

3.2. Dehydrogenation of isolated isomers

Further isolation of the two isomers was performed and mixtures containing enlarged amounts of one isomer were obtained. As these two mixtures, called HMR 1 (with 97% HMR 1 isomer) and HMR 2 (with 88% HMR 2 isomer) were used in the dehydrogenation reaction, it was obvious that HMR 2 reacted with higher reaction rate (Table 1). We have earlier concluded that HMR 2 reacted with higher rate also in the hydrogenolysis reaction to MAT [6,7]. The yield of oxoMAT was higher for HMR 2. Eklund and Sjöholm [4] concluded in the oxidation of HMR with DDQ, that the HMR 2 isomer gave oxoMAT but only small amounts were obtained when the HMR 1 isomer was used. It is visible from Table 1 that more of propoxyMAT 1 was obtained when HMR 1 was used, implying that HMR 1 and HMR 2 gave propoxyMAT 1 and propoxyMAT 2, respectively. This means that when Pd/CNF-400 and Pd/CNF-500 (the catalysts with the lowest concentration of acid sites) were used, HMR 1 formed more propoxyMAT 1 than when the most acidic catalysts were used (Fig. 3b) and consequently HMR 1 reacted with approximately the same overall rate as HMR 2 (which formed oxoMAT, MAT and propoxyMAT 2). This would then explain why the HMR 2-to-HMR 1 ratio did not change when Pd/CNF-400 and Pd/CNF-500 were used (Fig. 2c). A change in the HMR 2-to-HMR 1 ratio does not only have to be due to the difference in reaction rates for the two isomers, since the ratio also changes if HMR 2 isomerises to HMR 1. The isomerization from one isomer to another was observed in the hydrogenolysis of HMR [6,7,22], but in the dehydrogenation no clear evidence of isomerization was obtained.

The selectivity to oxoMAT can be further increased by using an alcohol with longer carbon chain as solvent. Table 1 shows that the yield of oxoMAT was the same for both 2-propanol

Table 1
Dehydrogenation of HMR isomers[a]

HMR isomer	Conversion[b]	Yield oxoMAT[c]	Yield MAT[d]	Yield propoxy 1[e]	Yield propoxy 2[f]
HMR 1[g]	0.45	0.14	0.09	0.19	0.03
HMR 2[h]	0.68	0.51	0.06	0.07	0.04
HMR 2[i]	0.56	0.51	0.05	0	0

[a] Conditions: 200 mg 0.99% Pd/CNF-300, 0.13 mmol of HMR isomer, 100 mL solvent, 70 °C, 100 mL/min N_2-flow (atmospheric pressure).
[b] Conversion of HMR at 4 h, conversion = $(c_{HMR,tot,0} - c_{HMR,tot})/c_{HMR,tot,0}$ ($0 \leq$ conversion ≤ 1).
[c] Yield of oxoMAT in 4 h ($0 \leq$ yield ≤ 1).
[d] Yield of MAT in 4 h ($0 \leq$ yield ≤ 1).
[e] Yield of propoxyMAT1 (the first isomer of 7-iso-propoxymatairesinol) in 4 h ($0 \leq$ yield ≤ 1).
[f] Yield of propoxyMAT2 (the second isomer of 7-iso-propoxymatairesinol) in 4 h ($0 \leq$ yield ≤ 1).
[g] The HMR mixture denoted HMR 1 contained 97% HMR 1 and 3% HMR 2. 2-Propanol was used as solvent.
[h] The HMR mixture denoted HMR 2 contained 12% HMR 1 and 88% HMR 2. 2-Propanol was used as solvent.
[i] The HMR mixture denoted HMR 2 contained 12% HMR 1 and 88% HMR 2. 2-Pentanol was used as solvent.

and 2-pentanol, but the amount of by-products decreased when 2-pentanol was used since no alkoxymatairesinol was formed.

3.3. Quantum chemical calculations

3.3.1. Properties of HMR 1 and HMR 2

The two HMR isomers were reacting with different reaction rates in the dehydrogenation and hydrogenolysis [6,7] reactions. If one of the HMR molecules has weaker bond strength or considerably different charge in the reactive hydroxyl group it could explain why the two isomers have different reaction rates. Therefore, theoretical calculations were performed: Mulliken and Löwdin charges, electrostatic potential fit (ESP) and bond orders as well as bond distances were calculated for the optimized molecules at the HF/6-31G* level. Only the charges of hydroxyl group oxygen (O12) and hydrogen (H12) as well as hydroxylcarbon (C7) are given in Table 2, while the numbering of the atoms is illustrated in Fig. 4. All relevant parameters are essentially the same for HMR 1 and HMR 2, when the most stable conformations (based on the electronic energy) determined in Ref. [25] were considered. The RRR_ue_4_B conformation of HMR 1 and the RRS_ue_3_B conformation of HMR 2 are shown in Fig. 5. The RRR_ue_4_B conformation is 2.7 kJ mol^{-1} (ΔG, 25 °C) more stable than the RRS_ue_3_B conformation.

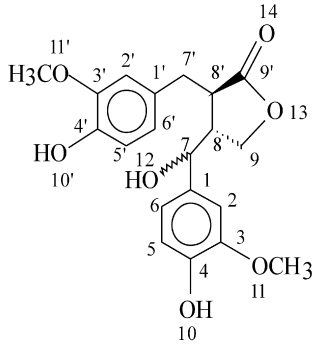

Fig. 4. Numbering of atoms in the HMR molecule.

3.3.2. Protonation

As the role of the Brønsted acid sites present on the catalyst support is apparent, based on the results presented above and in earlier studies [6,7], protonation of HMR 1 and HMR 2 was studied. Protonation has been proposed as the first step in the formation of MAT [6], as the acid sites play a major role in the reaction. The HMR molecule has seven potential proton acceptors, namely the oxygen atoms. Protonated forms of both molecules were studied by placing a proton close to all seven oxygen atoms. Besides protonation of the seven oxygen atoms, there is a possibility to form bifurcated bonding between the oxygen atoms O10 and O11 as well as between O10′ and O11′. The proton affinities were studied at the BP86/TZVP/MARI-*J* level. The protonation energy of a compound A is here defined as the negative electronic energy change for the reaction:

$$A + H^+ \rightarrow AH^+ \quad (1)$$

which can be understood as a proton affinity without thermodynamic contributions. When the proton was attached to

Table 2
Bond orders, bond distances and charges (Mulliken, Löwdin and ESP fits) for selected atoms of two HMR isomers

	Bond order C–O	Bond order O–H	Distance (pm), C–O	Distance (pm), O–H	Atom	Charge		
						Mulliken	Löwdin	ESP-fit
	0.86	0.76	140.3	94.8	C7	0.18	0.03	0.28
HMR1 RRR_ue_4_B					O12	−0.76	−0.51	−0.74
					H12	0.45	0.37	0.47
	0.85	0.76	140.9	94.8	C7	0.17	0.03	0.35
HMR2 RRS_ue_3_B					O12	−0.76	−0.51	−0.74
					H12	0.45	0.37	0.46

The code indicates the conformation taken from Ref. [25].

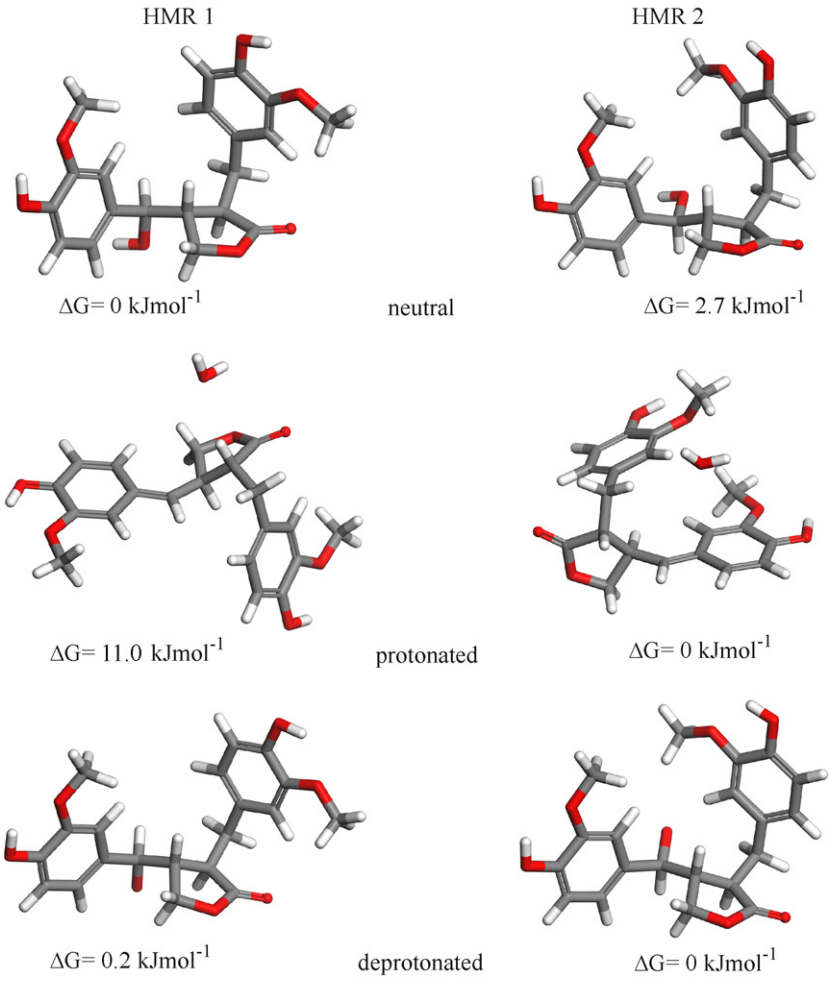

Fig. 5. B3LYP/TZVP optimized structures of neutral, protonated and deprotonated forms of HMR 1 and HMR 2.

oxygen atoms other than O12, the protonation energies varied between 800 and 909 kJ/mol for HMR 1 and between 785 and 909 kJ/mol for HMR 2 (adopting conformations RRR_ue_4_B and RRS_ue_3_B, respectively). The most stable structures were formed when the proton was attached to the hydroxyl oxygen O12, protonation energy being 911 and 915 kJ mol^{-1} for HMR 1 and HMR 2, respectively. However, when attaching the proton to O12 the optimization did not result in protonated HMR 1 or HMR 2 molecules, instead a water abstraction and consequently a complex of water molecule and carbenium ion was observed (see Fig. 5). In other words, protonation of the hydroxyl group leads to formation of a carbenium ion without any activation barrier. This is in line with the experiments as the corresponding hydroxyl group is the reactive one. The protonation was studied in detail at the B3LYP/TZVP level taking into account thermodynamic contributions, i.e. the Gibbs' free energy at 25 °C. After protonation and formation of water along with the carbenium ion complex, the formed complex of HMR 2 becomes 11.0 kJ mol^{-1} more stable than that of HMR 1. If these complexes are studied further and water is removed, i.e. only carbenium ions are considered, the carbenium ion formed from HMR 2 is 20.3 kJ mol^{-1} more stable than that formed from HMR 1. As water is removed carbon C7 becomes achiral, which means that the formed carbenium ions are only different conformations not different molecules as HMR 1 and HMR 2 are.

3.3.3. Deprotonation

Deprotonation followed by hydride abstraction is a possible mechanism for the formation of oxoMAT. The deprotonated structures of HMR 1 and HMR 2 were optimized at the B3LYP/TZVP level. The optimized structures are presented in Fig. 5. Both anions were observed to be equal in stability at 25 °C, i.e. the anion formed from HMR 2 is only 0.2 kJ mol^{-1} more stable than anion formed from HMR 1.

3.4. Reaction mechanisms for formation of oxoMAT

A reaction mechanism for the formation of MAT has already been presented in Ref. [6]. It was proposed that the initial step is protonation of the hydroxyl group followed by water abstraction and formation of a carbenium ionic intermediate. This is supported by the theoretical calculations performed in the present work. The formed carbenium ionic intermediate is then attacked by a hydride resulting in formation of MAT.

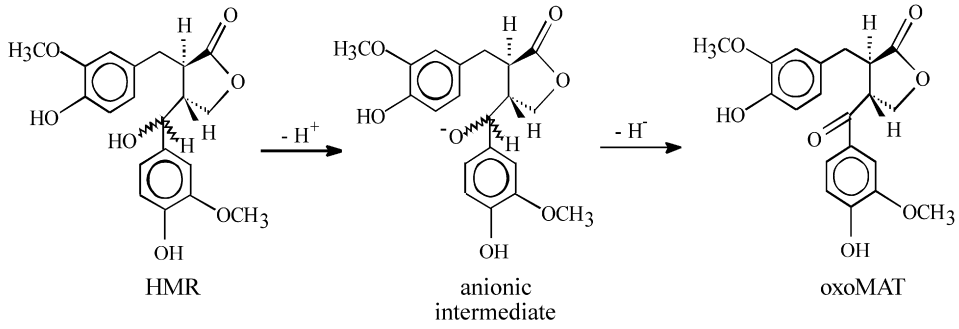

Fig. 6. Reaction mechanism for the dehydrogenation of HMR to oxoMAT.

The possible reaction mechanism for the formation of oxoMAT is presented in Fig. 6. The initial step is deprotonation of the hydroxyl group and formation of an anionic intermediate. The proton is most probably abstracted by the solvent 2-propanol, since aliphatic alcohols can function as bases [44] and the proton affinity for 2-propanol is approximately 100 kJ mol^{-1} lower than the proton affinity for HMR [45]. Next step is abstraction of hydride leading to formation of oxoMAT. The hydride could be removed from the molecule by palladium. It is known that hydrogen carries a negative charge in the palladium hydride and on the palladium surface [46]. Therefore it is logical to assume that the hydride is removed by palladium. The hydrogen, generated in the dehydrogenation reaction, can subsequently be used in the formation of MAT.

3.5. Reaction rates of HMR 1 and HMR 2

The theoretical calculations indicated that the explanation for the different dehydrogenation and hydrogenolysis rates of HMR 1 and HMR 2 is not due to the differences in the charges or bond strengths present in these molecules. The reason for different reaction rates is either the reaction intermediates formed or the interactions between the HMR isomers and catalyst surface. The quantum chemical calculations did not give any indication of the preferred anionic intermediate in the formation of oxoMAT. However, a correlation was found in the case of MAT formation. The protonation of the hydroxyl group at position C7 in HMR results in spontaneous abstraction of water and formation of carbenium ion. As the protonation of HMR 2 leads to a more stable complex and carbenium ion than protonation of HMR 1, formation of such carbenium ion (intermediate in the formation of MAT) is thermodynamically favoured. According to the Polayni relationship [47], a decrease in the energy for a reactant also decreases the activation energy, i.e. for a more stable intermediate the activation energy is lower and subsequently the reaction rate higher. This could explain why HMR 2 reacts to MAT with higher rate than HMR 1 [6,7].

Observe that the difference in stabilities between carbenium ions formed from HMR 1 and HMR 2 is rather indicative as the intermediates are not thoroughly studied here. Still, the effect of catalyst surface has not been taken into account in the calculations and excluding the surface may lead to false conclusions [48]. In any case, the calculations indicated that the formed intermediates (after protonation and deprotonation) from HMR 1 and HMR 2 might differ considerably from each other.

4. Conclusions

Carbon nanofibre supported palladium catalysts (Pd/CNF) were used in the dehydrogenation of hydroxymatairesinol (HMR, two diastereomers) to oxomatairesinol (oxoMAT), which is a potential anticarcinogenic and antioxidative compound. The concentration of acid sites on the catalyst surface was varied by heating at different temperatures under nitrogen flow. Both activity and selectivity to the desired product oxoMAT increased when the concentration of acid sites increased. Only one of the isomers gave oxoMAT as the major product. Quantum chemical calculations were performed as an attempt to explain this behaviour and a reaction mechanism for the dehydrogenation of HMR was proposed. HMR is first deprotonated giving an anionic intermediate, from which a hydride is abstracted to form oxoMAT. The major by-product was 7-i-propoxyMAT, which was formed through interactions with the solvent 2-propanol. Formation of this by-product can be suppressed and the selectivity to oxoMAT can subsequently be increased by choosing 2-pentanol as solvent.

Acknowledgements

This work is part of the activities at the Åbo Akademi Process Chemistry Centre within the Finnish Centre of Excellence Programme (2000–2011) by the Academy of Finland. Financial support from the Raisio Group Research Foundation and European Union through the Sixth Framework Programme (project 506621-1) are gratefully acknowledged. The authors express their gratitude to Mr. Christer Eckerman for the HMR preparation, Dr. Patrik Eklund for the separation of the isomers, and Mr. Markku Reunanen for GC–MS. V.N. thanks the Academy of Finland (project 212620) for financial support. Resources provided by CSC, the Finnish IT Center of Science, are kindly acknowledged.

References

[1] D.C. Ayres, J.D. Loike, Lignans—Chemical, Biological and Clinical Properties, Cambridge University Press, Cambridge, 1990, p. 1.

[2] S. Willför, J. Hemming, M. Reunanen, C. Eckerman, B. Holmbom, Holzforschung 57 (2003) 27–36.
[3] P.C. Eklund, F.J. Sundell, A.I. Smeds, R.E. Sjöholm, Org. Biomol. Chem. 2 (2004) 2229–2235.
[4] P.C. Eklund, R.E. Sjöholm, Tetrahedron 59 (2003) 4515–4523.
[5] P. Eklund, A. Lindholm, J.-P. Mikkola, A. Smeds, R. Lehtilä, R. Sjöholm, Org. Lett. 5 (2003) 491–493.
[6] H. Markus, P. Mäki-Arvela, N. Kumar, N.V. Kul'kova, P. Eklund, R. Sjöholm, B. Holmbom, T. Salmi, D.Yu. Murzin, Catal. Lett. 103 (2005) 125–131.
[7] H. Markus, P. Mäki-Arvela, N. Kumar, T. Heikkilä, V.-P. Lehto, R. Sjöholm, B. Holmbom, T. Salmi, D.Yu. Murzin, J. Catal. 238 (2006) 301–308.
[8] P. Eklund, R. Sillanpää, R. Sjöholm, J. Chem. Soc., Perkin Trans. 1 16 (2002) 1906–1910.
[9] H. Adlercreutz, Lancet 3 (2002) 364–373.
[10] S.M. Willför, M.O. Ahotupa, J.E. Hemming, M.H.T. Reunanen, P.C. Eklund, R.E. Sjöholm, C.S.E. Eckerman, S.P. Pohjamo, B.R. Holmbom, J. Agric. Food Chem. 51 (2003) 7600–7606.
[11] S. Yamauchi, T. Sugahara, Y. Nakashima, A. Okada, K. Akiyama, T. Kishida, M. Maruyama, T. Masuda, Biosci. Biotechnol. Biochem. 70 (2006) 1934–1940.
[12] P.C. Eklund, O.K. Långvik, J.P. Wärnå, T.O. Salmi, S.M. Willför, R.E. Sjöholm, Org. Biomol. Chem. 3 (2005) 3336–3347.
[13] F. Kawamura, M. Miyachi, S. Kaway, J. Wood Sci. 44 (1998) 47–55.
[14] K.P. de Jong, J.W. Geus, Catal. Rev. Sci. Eng. 42 (2000) 481–510.
[15] P. Serp, M. Corrias, P. Kalck, Appl. Catal. A 253 (2003) 337–358.
[16] M.K. van der Lee, A.J. van Dillen, J.W. Geus, K.P. de Jong, J.H. Bitter, Carbon 44 (2006) 629–637.
[17] T.G. Ros, D.E. Keller, A.J. van Dillen, J.W. Geus, D.C. Koningsberger, J. Catal. 211 (2002) 85–102.
[18] T. Mallat, A. Baiker, Chem. Rev. 104 (2004) 3037–3058.
[19] M. Besson, P. Gallezot, Catal. Today 57 (2000) 127–141.
[20] F. Zaccheria, N. Ravasio, R. Psaro, A. Fusi, Chem. Commun. (2005) 253–255.
[21] C. Keresszegi, T. Mallat, A. Baiker, New J. Chem. 25 (2001) 1163–1167.
[22] H. Markus, A.J. Plomp, P. Mäki-Arvela, J.H. Bitter, D.Yu. Murzin, Catal. Lett. 113 (2007) 141–146.
[23] M.L. Toebes, J.H. Bitter, A.J. van Dillen, K.P. de Jong, Catal. Today 76 (2002) 33–42.
[24] F. Winter, A.J. van Dillen, K.P. de Jong, J. Mol. Catal. A 219 (2004) 273–281.
[25] A. Taskinen, P. Eklund, R. Sjöholm, M. Hotokka, J. Mol. Struct. 677 (2004) 113–124.
[26] M.W. Schmidt, K.K. Baldridge, J.A. Boatz, S.T. Elbert, M.S. Gordon, J.H. Jensen, S. Koseki, N. Matsunaga, K.A. Nguyen, S.J. Su, T.L. Windus, M. Dupuis, J.A. Montgomery, J. Comput. Chem. 14 (1993) 1347–1363.
[27] W.J. Hehre, L. Radom, P.V.R. Schleyer, J.A. Pople, Ab Initio Molecular Orbital Theory, John Wiley & Sons, New York, 1986.
[28] W.J. Hehre, R. Ditchfield, J.A. Pople, J. Chem. Phys. 56 (1972) 2257–2261.
[29] P.C. Hariharan, J.A. Pople, Theor. Chim. Acta 28 (1973) 213–222.
[30] M.M. Francl, W.J. Pietro, W.J. Hehre, J.S. Binkley, D.J. DeFrees, J.A. Pople, M.S. Gordon, J. Chem. Phys. 77 (1982) 3654–3665.
[31] R. Ahlrichs, M. Bär, M. Häser, H. Horn, C. Kölmel, Chem. Phys. Lett. 162 (1989) 165–169.
[32] M. Häser, R. Ahlrichs, J. Comput. Chem. 10 (1989) 104–111.
[33] M. von Arnim, R. Ahlrichs, J. Comput. Chem. 19 (1998) 1746–1757.
[34] A.D. Becke, Phys. Rev. A 38 (1988) 3098–3100.
[35] J.P. Perdew, Phys. Rev. B 33 (1986) 8822–8824.
[36] K. Eichkorn, O. Treutler, H. Öhm, M. Häser, R. Ahlrichs, Chem. Phys. Lett. 242 (1995) 652–660.
[37] K. Eichkorn, F. Weigend, O. Treutler, R. Ahlrichs, Theor. Chem. Acc. 97 (1997) 119–124.
[38] M. Sierka, A. Hogekamp, R. Ahlrichs, J. Chem. Phys. 118 (2003) 9136–9148.
[39] A. Schäfer, C. Huber, R. Ahlrichs, J. Chem. Phys. 100 (1994) 5829–5835.
[40] C. Lee, W. Yang, R.G. Parr, Phys. Rev. B 37 (1988) 785–789.
[41] A.D. Becke, J. Chem. Phys. 98 (1993) 5648–5652.
[42] A. Scott, L. Radom, J. Phys. Chem. 100 (1996) 16502–16513.
[43] D. Parra, J.F. Izquierdo, F. Cunill, J. Tejero, C. Fité, M. Iborra, M. Vila, Ind. Eng. Chem. Res. 37 (1998) 3575–3581.
[44] D.G. Lee, R. Cameron, J. Am. Chem. Soc. 93 (1971) 4724–4728.
[45] V.V. Brei, D.V. Shistka, A.G. Grebenyuk, Theor. Exp. Chem. 40 (2004) 192–197.
[46] L.L. Jewell, B.H. Davis, Appl. Catal. A 310 (2006) 1–15.
[47] R.I. Masel, Principles of Adsorption and Reaction on Solid Surfaces, John Wiley & Sons Inc., New York, 1996, p. 621.
[48] V. Nieminen, A. Taskinen, E. Toukoniitty, M. Hotokka, D.Yu. Murzin, J. Catal. 237 (2006) 131–142.